Meccanica (2021) 56:1505–1521
https://doi.org/10.1007/s11012-020-01179-1

On the two-potential constitutive modeling of dielectric elastomers

Kamalendu Ghosh · Oscar Lopez-Pamies

Received: 18 January 2020 / Accepted: 14 May 2020 / Published online: 8 June 2020

Abstract This work lays out the two-potential framework for the constitutive modeling of dielectric elastomers. After its general presentation, where the constraints imposed by even electromechanical coupling, material frame indifference, material symmetry, and entropy imbalance are all spelled out, the framework is utilized to put forth a specific constitutive model for the prominent class of isotropic incompressible dielectric elastomers. The model accounts for the non-Gaussian elasticity and electrostriction typical of such materials, as well as for their deformation-enhanced shear thinning due to viscous dissipation and their time-dependent polarization due to electric dissipation. The key theoretical and practical features of the model are discussed, with special emphasis on its specialization in the limit of small deformations and moderate electric fields. The last part of this paper is devoted to the deployment of the model to fully describe the electromechanical behavior of a commercially significant dielectric elastomer, namely, the acrylate elastomer VHB 4910 from 3M.

Keywords Finite deformations · Electrostriction · Dissipative solids · Internal variables

K. Ghosh · O. Lopez-Pamies (✉)
Department of Civil and Environmental Engineering, University of Illinois, Urbana–Champaign, IL 61801-2352, USA
e-mail: pamies@illinois.edu

1 Introduction

Over the last two decades, fueled by their potential to enable a broad spectrum of new technologies ranging from soft robots, to energy harvesters, to speakers, to biomedical and haptic devices [3, 6, 15, 36, 49], increasing efforts have been devoted to gain precise quantitative insight into the electromechanical behavior of dielectric elastomers.

On the theoretical front, most of the reported efforts have restricted attention to the idealization that dielectric elastomers are *elastic dielectrics*, that is, materials that deform and polarize without incurring dissipation of energy [9, 11, 27, 28, 32, 34, 43]. While such an idealization may be justified under certain loading conditions, it is not appropriate in general as dielectric elastomers are inherently dissipative solids: they dissipate energy through viscous deformation and through friction in their electric polarization process.

Recognizing their true nature, a handful of dissipative models have been proposed over the last decade following different *ad hoc* approaches. The majority of such models account only for mechanical—and *not* for electric—dissipation and, save for a few works [5, 46], most assume ideal dielectric behavior [2, 18, 47, 51]. The motivation for this bias is that the mechanical relaxation time of dielectric elastomers is much larger that their electric relaxation time. Yet, accounting for electric dissipation, in addition to mechanical dissipation, is critical when dealing with applied alternating currents, which is often the case in

applications. Two exemptions that account for both mechanical and electric dissipation are the models presented in [10] and [38]. The former corresponds to a model for the special case of a non-ideal dielectric elastomer with Gaussian elasticity, constant viscosity, and a single relaxation time due to electric dissipation. The latter corresponds to a model for a different special case, that of an ideal dielectric elastomer with non-Gaussian elasticity, also constant viscosity, and an *ad hoc* electric dissipation attributed to leakage current that is strictly applicable to a one-dimensional setting. In this context, our purpose in this paper is threefold.

First, we introduce a general constitutive framework to construct models for the dissipative electromechanical behavior of dielectric elastomers that automatically feature the distinguishing even electromechanical coupling of this class of materials as well as seamlessly comply with material frame indifference, material symmetry, and the entropy imbalance requirements. As elaborated in Sect. 2, this framework is nothing more than the celebrated two-potential framework in mechanics [13, 16, 24, 53, 54] extended to account for the coupling with Maxwell's equations.

Second, we make use of the general two-potential framework to construct a specific model for the prominent class of isotropic and incompressible dielectric elastomers. As elaborated in Sect. 3, the proposed model corresponds to a generalization of the rubber viscoelastic model of Kumar and Lopez-Pamies [24]. Accordingly, it accounts for the non-Gaussian elasticity and the deformation-enhanced shear-thinning viscosity typical of dielectric elastomers. It also accounts for their characteristic electrostriction and time- and deformation-dependent polarization. Section 3 also includes a detailed analysis of the specialization of the model in the fundamental limit of small deformations and moderate electric fields.

Third, for demonstration purposes, we deploy the proposed model to describe the electromechanical behavior of the acrylate elastomer VHB 4910 in full. As illustrated in Sect. 4 by means of direct comparisons with experimental data available in the literature, the model is capable both of describing and predicting the electromechanical behavior of this popular and commercially significant dielectric elastomer from 3M.

2 The two-potential framework for dielectric elastomers

2.1 Kinematics

Consider a deformable and polarizable homogeneous solid that occupies in its initial—undeformed, stress-free, and unpolarized—configuration (at time $t = 0$) an open bounded domain $\Omega_0 \subset \mathbb{R}^3$, with boundary $\partial\Omega_0$ and unit outward normal $\mathbf{N}$. We identify material points by their initial position vector $\mathbf{X} \in \Omega_0$. At a later time $t \in (0, T]$, due to the applied boundary conditions and source terms described below, the position vector $\mathbf{X}$ of a material point moves to a new position specified by

$$\mathbf{x} = \mathbf{y}(\mathbf{X}, t),$$

where $\mathbf{y}$ is an invertible mapping from Ω_0 to the current configuration $\Omega(t)$, also contained in $\mathbb{R}^3$. We write the associated deformation gradient and its determinant at $\mathbf{X}$ and t as

$$\mathbf{F} = \nabla\mathbf{y}(\mathbf{X}, t) = \frac{\partial \mathbf{y}}{\partial \mathbf{X}}(\mathbf{X}, t) \quad \text{and} \quad J = \det \mathbf{F}.$$

2.2 Constitutive behavior

Following the two-potential formalism [13, 16, 24, 53, 54], absent changes in temperature, the constitutive behavior of the solid can be expediently characterized by two thermodynamic potentials that describe how the solid *stores* and *dissipates* energy through deformation and polarization, namely: (*i*) a free-energy function ψ and (*ii*) a dissipation potential ϕ.

The functional form of these two potentials must be selected so as to be descriptive of the three basic defining features of dielectric elastomers, to wit:

- dielectric elastomers exhibit even electromechanical coupling,
- when all mechanical forces and electric fields are removed after an arbitrary loading path, dielectric elastomers creep to their original undeformed, stress-free, and unpolarized initial configuration, and
- when subject to mechanical (electric) relaxation and creep loading conditions, dielectric elastomers exhibit a transient response that then evolves into

an equilibrium state of deformation (voltage) and stress (polarization).

The last two of the above defining features dictate the following functional form:

$$\psi = \psi^{\mathrm{Eq}}(\mathbf{F}, \mathbf{E}) + \psi^{\mathrm{NEq}}(\mathbf{F}, \mathbf{E}, \mathbf{F}\mathbf{F}^{v-1}, \mathbf{E} - \mathbf{E}^{v}) \tag{1}$$

for the free-energy function and

$$\phi = \phi(\mathbf{F}, \mathbf{E}, \mathbf{F}^{v}, \mathbf{E}^{v}, \dot{\mathbf{F}}^{v}, \dot{\mathbf{E}}^{v}) \tag{2}$$

for the dissipation potential; the first feature is summoned further below in Sect. 2.2.1 together with other fundamental constraints that the functions ψ and ϕ ought to satisfy. In relation (1), ψ^{Eq} characterizes the energy storage in the dielectric elastomer at states of mechanical and electric (i.e., thermodynamic) equilibrium, while ψ^{NEq} characterizes the additional energy storage at non-equilibrium states (i.e., the part of the energy that gets dissipated eventually). Accordingly, the former is a function solely of the deformation gradient $\mathbf{F}$ and the Lagrangian electric field[1] $\mathbf{E}$. On the other hand, the function ψ^{NEq} depends on $\mathbf{F}$, $\mathbf{E}$, and additionally on the internal variables $\mathbf{F}^{v}$ and $\mathbf{E}^{v}$ via the combinations

$$\mathbf{F}^{e} := \mathbf{F}\mathbf{F}^{v-1} \quad \text{and} \quad \mathbf{E}^{e} := \mathbf{E} - \mathbf{E}^{v}.$$

In relation (2), the variables $\dot{\mathbf{F}}^{v}$ and $\dot{\mathbf{E}}^{v}$ stand for the time derivatives of the internal variables, that is, $\dot{\mathbf{F}}^{v} = \partial\mathbf{F}^{v}(\mathbf{X}, t)/\partial t$ and $\dot{\mathbf{E}}^{v} = \partial\mathbf{E}^{v}(\mathbf{X}, t)/\partial t$.

Remark 1 The specific choice of internal variables $\mathbf{F}^{v}$ and $\mathbf{E}^{v}$ in the formulation (1)–(2) is one among several possible *constitutive* choices. It is a choice, nonetheless, that has the advantages of being amply general and yet mathematically simple and of having a clear physical meaning. Indeed, $\mathbf{F}^{v}$ and $\mathbf{E}^{v}$ stand for measures of the "dissipative parts" of the deformation gradient $\mathbf{F}$ and the electric field $\mathbf{E}$. They are consistent with standard and well-tested choices in the separate literatures of mechanics and dielectrics; see, e.g., [24, 33, 39].

Remark 2 In the spirit of the classical linear theories of viscoelasticity [14] and time-dependent dielectrics [4], it proves instructive to visualize the physical meaning of the two potentials (1) and (2) pictorially in the form of an electrorheological model. Figure 1 provides such a representation, which can be readily identified as the classical Zener model for viscoelastic solids [50] and the Debye model for dielectrics [8] generalized to account for their electromechanical coupling as well as for the constitutive and geometric nonlinearities inherent at finite deformations and finite electric fields.

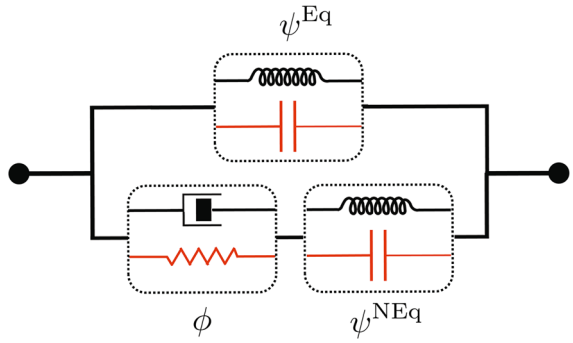

Fig. 1 Electrorheological model of dielectric elastomers. The curly coils and parallel plates represent elastic springs and capacitors, while the dashpot and sharp coil represent a viscous dashpot and a resistor. The elastic springs and capacitors symbolize the ability of dielectric elastomers to store elastic and electric energy, while the viscous dashpot and resistor symbolize their ability to dissipate energy through viscous deformation and molecular friction during their polarization

Granted the two potentials (1) and (2), it follows that the "total" first Piola–Kirchhoff stress tensor $\mathbf{S}$ (accounting for both, the mechanical and electric contributions [9]) and the Lagrangian electric displacement $\mathbf{D}$ at any material point $\mathbf{X} \in \Omega_0$ and time $t \in [0, T]$ are given by the relations

$$\mathbf{S}(\mathbf{X}, t) = \frac{\partial\psi^{\mathrm{Eq}}}{\partial\mathbf{F}} + \frac{\partial\psi^{\mathrm{NEq}}}{\partial\mathbf{F}} \tag{3}$$

and

$$\mathbf{D}(\mathbf{X}, t) = -\frac{\partial\psi^{\mathrm{Eq}}}{\partial\mathbf{E}} - \frac{\partial\psi^{\mathrm{NEq}}}{\partial\mathbf{E}}, \tag{4}$$

where $\mathbf{F}^{v}(\mathbf{X}, t)$ and $\mathbf{E}^{v}(\mathbf{X}, t)$ are defined implicitly as solutions of the coupled system of ordinary differential equations (ODEs)

$$\begin{cases} \dfrac{\partial\psi^{\mathrm{NEq}}}{\partial\mathbf{F}^{v}} + \dfrac{\partial\phi}{\partial\dot{\mathbf{F}}^{v}} = 0 \\ \dfrac{\partial\psi^{\mathrm{NEq}}}{\partial\mathbf{E}^{v}} + \dfrac{\partial\phi}{\partial\dot{\mathbf{E}}^{v}} = 0 \end{cases} \tag{5}$$

[1] In this paper, for definiteness, we restrict attention to the Lagrangian electric field $\mathbf{E}$ as the independent electric variable.

in time subject to the initial conditions $\mathbf{F}^v(\mathbf{X},0)=\mathbf{I}$ and $\mathbf{E}^v(\mathbf{X},0)=\mathbf{0}$.

Remark 3 The total Cauchy stress tensor $\mathbf{T}$, Eulerian electric field $\mathbf{e}$, and Eulerian electric displacement $\mathbf{d}$ at the position $\mathbf{x}\in\Omega(t)$ occupied by the material point $\mathbf{X}$ at time $t\in[0,T]$ are given in terms of their Lagrangian counterparts by the relations

$$\begin{aligned}\mathbf{T}(\mathbf{x},t)&=J^{-1}\mathbf{S}\mathbf{F}^T,\\ \mathbf{e}(\mathbf{x},t)&=\mathbf{F}^{-T}\mathbf{E},\\ \mathbf{d}(\mathbf{x},t)&=J^{-1}\mathbf{F}\mathbf{D}.\end{aligned}\tag{6}$$

Moreover, the polarization $\mathbf{p}$ at any $\mathbf{x}\in\Omega(t)$ and $t\in[0,T]$ is given by

$$\mathbf{p}(\mathbf{x},t)=\mathbf{d}(\mathbf{x},t)-\varepsilon_0\mathbf{e}(\mathbf{x},t),$$

where ε_0 stands for the permittivity of vacuum.

2.2.1 Constraints on the functions ψ^{Eq}, ψ^{NEq}, ϕ

As is the case with the two-potential modeling of any dissipative solid, any specific choice of functions ψ^{Eq}, ψ^{NEq}, ϕ in the formulation (1)–(2) must satisfy certain basic physical requirements. We spell out each of these requirements in the sequel, one at a time.

Even electromechanical coupling. As alluded to above, the constitutive relations (3)–(4) for dielectric elastomers must exhibit even electromechanical coupling. This requirement implies that the functions ψ^{Eq}, ψ^{NEq}, ϕ must satisfy the conditions

$$\begin{aligned}&\psi^{\mathrm{Eq}}(\mathbf{F},-\mathbf{E})=\psi^{\mathrm{Eq}}(\mathbf{F},\mathbf{E}),\\ &\psi^{\mathrm{NEq}}(\mathbf{F},-\mathbf{E},\mathbf{F}^e,-\mathbf{E}^e)=\psi^{\mathrm{NEq}}(\mathbf{F},\mathbf{E},\mathbf{F}^e,\mathbf{E}^e),\\ &\phi(\mathbf{F},-\mathbf{E},\mathbf{F}^v,-\mathbf{E}^v,\dot{\mathbf{F}}^v,-\dot{\mathbf{E}}^v)=\phi(\mathbf{F},\mathbf{E},\mathbf{F}^v,\mathbf{E}^v,\dot{\mathbf{F}}^v,\dot{\mathbf{E}}^v),\end{aligned}\tag{7}$$

for arbitrary $\mathbf{F}$, $\mathbf{E}$, $\mathbf{F}^v$, and $\mathbf{E}^v$.

Material frame indifference. Under a change of observer, it is required that the free-energy function ψ and dissipation potential ϕ remain invariant. A standard calculation shows (see, e.g., Section 2 in [24]) that this requirement implies that the functions ψ^{Eq}, ψ^{NEq}, ϕ must satisfy the conditions

$$\begin{aligned}&\psi^{\mathrm{Eq}}(\mathbf{Q}\mathbf{F},\mathbf{E})=\psi^{\mathrm{Eq}}(\mathbf{F},\mathbf{E}),\\ &\psi^{\mathrm{NEq}}(\mathbf{Q}\mathbf{F},\mathbf{E},\mathbf{Q}\mathbf{F}^e,\mathbf{E}^e)=\psi^{\mathrm{NEq}}(\mathbf{F},\mathbf{E},\mathbf{F}^e,\mathbf{E}^e),\\ &\phi(\mathbf{Q}\mathbf{F},\mathbf{E},\mathbf{F}^v,\mathbf{E}^v,\dot{\mathbf{F}}^v,\dot{\mathbf{E}}^v)=\phi(\mathbf{Q}\mathbf{F},\mathbf{E},\mathbf{F}^v,\mathbf{E}^v,\dot{\mathbf{F}}^v,\dot{\mathbf{E}}^v)\end{aligned}\tag{8}$$

for all $\mathbf{Q}\in Orth^+$ and arbitrary $\mathbf{F}$, $\mathbf{E}$, $\mathbf{F}^v$, and $\mathbf{E}^v$.

Material symmetry. For dielectric elastomers with material symmetry group $Symm\subseteq Orth^+$, it is required that the free-energy function ψ and dissipation potential ϕ remain invariant under a change of reference configuration described by any element $\mathbf{K}\in Symm$. Again, a standard calculation shows (see, e.g., Section 2 in [24]) that this requirement implies that the functions ψ^{Eq}, ψ^{NEq}, ϕ must satisfy the conditions

$$\begin{aligned}&\psi^{\mathrm{Eq}}(\mathbf{F}\mathbf{K},\mathbf{K}^T\mathbf{E})=\psi^{\mathrm{Eq}}(\mathbf{F},\mathbf{E}),\\ &\psi^{\mathrm{NEq}}(\mathbf{F}\mathbf{K},\mathbf{K}^T\mathbf{E},\mathbf{F}^e,\mathbf{K}^T\mathbf{E}^e)=\psi^{\mathrm{NEq}}(\mathbf{F},\mathbf{E},\mathbf{F}^e,\mathbf{E}^e),\\ &\phi(\mathbf{F}\mathbf{K},\mathbf{K}^T\mathbf{E},\mathbf{F}^v\mathbf{K},\mathbf{K}^T\mathbf{E}^v,\dot{\mathbf{F}}^v\mathbf{K},\mathbf{K}^T\dot{\mathbf{E}}^v)\\ &=\phi(\mathbf{F},\mathbf{E},\mathbf{F}^v,\mathbf{E}^v,\dot{\mathbf{F}}^v,\dot{\mathbf{E}}^v)\end{aligned}\tag{9}$$

for all $\mathbf{K}\in Symm$ and arbitrary $\mathbf{F}$, $\mathbf{E}$, $\mathbf{F}^v$, and $\mathbf{E}^v$; in the condition for ψ^{NEq}, note that use has been made of the result $\mathbf{F}\mathbf{K}(\mathbf{F}^v\mathbf{K})^{-1}=\mathbf{F}\mathbf{K}\mathbf{K}^T\mathbf{F}^{v-1}=\mathbf{F}\mathbf{F}^{v-1}=\mathbf{F}^e$.

Entropy imbalance. In the context of isothermal processes of interest here, the entropy imbalance or second law of thermodynamics in the form of the reduced dissipation inequality (see the Appendix) imposes the following constraint on the dissipation potential ϕ:

$$\begin{aligned}&\left[\frac{\partial\phi}{\partial\dot{\mathbf{F}}^v}(\mathbf{F},\mathbf{E},\mathbf{F}^v,\mathbf{E}^v,\dot{\mathbf{F}}^v,\dot{\mathbf{E}}^v)\right]\cdot\dot{\mathbf{F}}^v+\\ &\left[\frac{\partial\phi}{\partial\dot{\mathbf{E}}^v}(\mathbf{F},\mathbf{E},\mathbf{F}^v,\mathbf{E}^v,\dot{\mathbf{F}}^v,\dot{\mathbf{E}}^v)\right]\cdot\dot{\mathbf{E}}^v\geq 0\end{aligned}\tag{10}$$

for arbitrary $\mathbf{F}$, $\mathbf{E}$, $\mathbf{F}^v$, $\mathbf{E}^v$, with equality holding only when $\dot{\mathbf{F}}^v=\mathbf{0}$ and $\dot{\mathbf{E}}^v=\mathbf{0}$.

2.3 Boundary conditions and source terms

We now specify the external stimuli applied to the solid, which comprise both prescribed mechanical and electric boundary data and source terms in the bulk.

Electrically, consistent with the manner in which electric fields are applied in practice, we take that the solid is immersed in a surrounding space (e.g., air)

where there is a heterogeneous electric field $\overline{\mathbf{E}}(\mathbf{X},t)$ and corresponding electric displacement $\overline{\mathbf{D}}(\mathbf{X},t)$ that result from the electrodes connected to part of the boundary of the solid together with the nearby presence of space charges and/or other polarizable bodies and the interaction of these with the solid. We can then compactly write the boundary condition as

$$\mathbf{E}\times\mathbf{N}=\overline{\mathbf{E}}\times\mathbf{N},\quad (\mathbf{X},t)\in\partial\Omega_0\times[0,T]$$

or, equivalently,

$$\mathbf{D}\cdot\mathbf{N}=\overline{\mathbf{D}}\cdot\mathbf{N}-\sigma(\mathbf{X},t),\quad (\mathbf{X},t)\in\partial\Omega_0\times[0,T]$$

over the entirety of the boundary of the domain occupied by the solid, where $\sigma(\mathbf{X},t)$ stands for the density of surface charges present on $\partial\Omega_0$ (for instance, at electrodes). Throughout Ω_0, we also consider that the solid contains a distribution of space charges with density

$$Q(\mathbf{X},t),\quad (\mathbf{X},t)\in\Omega_0\times[0,T].$$

Mechanically, on a portion $\partial\Omega_0^{\mathcal{D}}$ of the boundary $\partial\Omega_0$, the deformation field $\mathbf{y}$ is taken to be given by a known function $\overline{\mathbf{y}}(\mathbf{X},t)$, while the complementary part of the boundary $\partial\Omega_0^{\mathcal{N}}=\partial\Omega_0\setminus\partial\Omega_0^{\mathcal{D}}$ is subjected to a prescribed mechanical traction $\overline{\mathbf{t}}(\mathbf{X},t)$. Precisely,

$$\begin{cases}\mathbf{y}=\overline{\mathbf{y}}, & (\mathbf{X},t)\in\partial\Omega_0^{\mathcal{D}}\times[0,T]\\ \mathbf{S}\mathbf{N}=\overline{\mathbf{t}}+\mathbf{S}_M\mathbf{N}, & (\mathbf{X},t)\in\partial\Omega_0^{\mathcal{N}}\times[0,T].\end{cases}$$

In this last expression, $\mathbf{S}_M$ stands for the Maxwell stress outside of the solid. In the case when the solid is surrounded by air,

$$\mathbf{S}_M=\overline{\mathbf{F}}^{-T}\overline{\mathbf{E}}\otimes\overline{\mathbf{D}}-\frac{\overline{J}\varepsilon_0}{2}\left(\mathbf{F}^{-T}\overline{\mathbf{E}}\cdot\overline{\mathbf{F}}^{-T}\overline{\mathbf{E}}\right)\overline{\mathbf{F}}^{-T},$$

where $\overline{\mathbf{D}}=\varepsilon_0\overline{J}\,\overline{\mathbf{F}}^{-1}\overline{\mathbf{F}}^{-T}\overline{\mathbf{E}}$ and where we emphasize that the meaning of the deformation gradient $\overline{\mathbf{F}}$—as well as the notion of material points $\mathbf{X}$—in the air needs to be interpreted appropriately; see, e.g., Section 6 in [29]. Finally, throughout Ω_0, we also consider that the solid is subjected to a mechanical body force with density

$$\mathbf{f}(\mathbf{X},t),\quad (\mathbf{X},t)\in\Omega_0\times[0,T].$$

2.4 Governing equations

Absent inertia and in the context of electro-quasi-statics, the relevant equations of balance of linear and angular momenta read as

$$\operatorname{Div}\mathbf{S}+\mathbf{f}=\mathbf{0}\quad\text{and}\quad\mathbf{S}\mathbf{F}^T=\mathbf{F}\mathbf{S}^T,\quad(\mathbf{X},t)\in\Omega_0\times[0,T]\tag{11}$$

while the relevant equations of Maxwell read as

$$\operatorname{Div}\mathbf{D}=Q\quad\text{and}\quad\operatorname{Curl}\mathbf{E}=\mathbf{0},\quad(\mathbf{X},t)\in\mathbb{R}^3\times[0,T].\tag{12}$$

The balance of angular momentum $(11)_2$ is automatically satisfied by virtue of the material frame indifference granted by condition $(8)_{1,2}$. Faraday's law $(12)_2$ can also be automatically satisfied by introducing a scalar potential φ such that $\mathbf{E}=-\nabla\varphi(\mathbf{X},t)$. It then follows that the governing equations for the solid reduce to the following coupled system of boundary-value problems:

$$\begin{cases}\operatorname{Div}\left[\dfrac{\partial\psi^{\mathrm{Eq}}}{\partial\mathbf{F}}(\nabla\mathbf{y},-\nabla\varphi)+\dfrac{\partial\psi^{\mathrm{NEq}}}{\partial\mathbf{F}}\left(\nabla\mathbf{y},-\nabla\varphi,\nabla\mathbf{y}\mathbf{F}^{v-1},-\nabla\varphi-\mathbf{E}^v\right)\right]+\mathbf{f}(\mathbf{X},t)=\mathbf{0},\quad(\mathbf{X},t)\in\Omega_0\times[0,T]\\ \det\nabla\mathbf{y}(\mathbf{X},t)>0,\quad(\mathbf{X},t)\in\Omega_0\times[0,T]\\ \mathbf{y}(\mathbf{X},t)=\overline{\mathbf{y}}(\mathbf{X},t),\quad(\mathbf{X},t)\in\partial\Omega_0^{\mathcal{D}}\times[0,T]\\ \left[\dfrac{\partial\psi^{\mathrm{Eq}}}{\partial\mathbf{F}}(\nabla\mathbf{y},-\nabla\varphi)+\dfrac{\partial\psi^{\mathrm{NEq}}}{\partial\mathbf{F}}\left(\nabla\mathbf{y},-\nabla\varphi,\nabla\mathbf{y}\mathbf{F}^{v-1},-\nabla\varphi-\mathbf{E}^v\right)-\mathbf{S}_M\right]\mathbf{N}=\overline{\mathbf{t}}(\mathbf{X},t),\ (\mathbf{X},t)\in\partial\Omega_0^{\mathcal{N}}\times[0,T]\end{cases}\tag{13}$$

and

$$\begin{cases} \mathrm{Div}\left[\dfrac{\partial\psi^{\mathrm{Eq}}}{\partial\mathbf{E}}(\nabla\mathbf{y},-\nabla\varphi)+\dfrac{\partial\psi^{\mathrm{NEq}}}{\partial\mathbf{E}}\left(\nabla\mathbf{y},-\nabla\varphi,\nabla\mathbf{y}\mathbf{F}^{v-1},-\nabla\varphi-\mathbf{E}^{v}\right)\right]=-Q(\mathbf{X},t), \quad (\mathbf{X},t)\in\Omega_0\times[0,T] \\ \left[\dfrac{\partial\psi^{\mathrm{Eq}}}{\partial\mathbf{E}}(\nabla\mathbf{y},-\nabla\varphi)+\dfrac{\partial\psi^{\mathrm{NEq}}}{\partial\mathbf{E}}\left(\nabla\mathbf{y},-\nabla\varphi,\nabla\mathbf{y}\mathbf{F}^{v-1},-\nabla\varphi-\mathbf{E}^{v}\right)\right]\cdot\mathbf{N}=\sigma(\mathbf{X},t)-\overline{\mathbf{D}}(\mathbf{X},t)\cdot\mathbf{N}, \ (\mathbf{X},t)\in\partial\Omega_0\times[0,T] \end{cases} \tag{14}$$

together with the coupled system of evolution equations

$$\begin{cases} \dfrac{\partial\psi^{\mathrm{NEq}}}{\partial\mathbf{F}^{v}}\left(\nabla\mathbf{y},-\nabla\varphi,\nabla\mathbf{y}\mathbf{F}^{v-1},-\nabla\varphi-\mathbf{E}^{v}\right)+\dfrac{\partial\phi}{\partial\dot{\mathbf{F}}^{v}}\left(\nabla\mathbf{y},-\nabla\varphi,\mathbf{F}^{v},\mathbf{E}^{v},\dot{\mathbf{F}}^{v},\dot{\mathbf{E}}^{v}\right)=0, \quad (\mathbf{X},t)\in\Omega_0\times(0,T] \\ \mathbf{F}^{v}(\mathbf{X},0)=\mathbf{I}, \quad \mathbf{X}\in\Omega_0 \end{cases} \tag{15}$$

and

$$\begin{cases} \dfrac{\partial\psi^{\mathrm{NEq}}}{\partial\mathbf{E}^{v}}\left(\nabla\mathbf{y},-\nabla\varphi,\nabla\mathbf{y}\mathbf{F}^{v-1},-\nabla\varphi-\mathbf{E}^{v}\right)+\dfrac{\partial\phi}{\partial\dot{\mathbf{E}}^{v}}\left(\nabla\mathbf{y},-\nabla\varphi,\mathbf{F}^{v},\mathbf{E}^{v},\dot{\mathbf{F}}^{v},\dot{\mathbf{E}}^{v}\right)=0, \quad (\mathbf{X},t)\in\Omega_0\times(0,T] \\ \mathbf{E}^{v}(\mathbf{X},0)=\mathbf{0}, \quad \mathbf{X}\in\Omega_0 \end{cases} \tag{16}$$

for the deformation field $\mathbf{y}(\mathbf{X},t)$, the electric potential $\varphi(\mathbf{X},t)$, and the internal variables $\mathbf{F}^{v}(\mathbf{X},t)$ and $\mathbf{E}^{v}(\mathbf{X},t)$.

Remark 4 In general, the boundary data $\overline{\mathbf{D}}(\mathbf{X},t)$ in $(14)_2$ is *not* known a priori. This is because it is implicitly defined by the solution of Maxwell equations (12) in $\mathbb{R}^3\setminus\Omega_0$. Nevertheless, there is a plurality of specific domain geometries Ω_0 and specific boundary conditions of practical interest for which the boundary condition $(14)_2$ can be written in explicit form, often in terms of an electric potential or voltage applied across electrodes.

Remark 5 The two-potential framework introduced above is admittedly general, as it applies to dielectric elastomers of arbitrary anisotropy and compressibility featuring a wide range of dissipative mechanical and electric behaviors, and yet relatively simple, as the resulting governing equations (13)–(14) with (15)–(16) for any boundary-value problem of interest are amenable to numerical solution by well-established finite-element and time-integration schemes; see, e.g., [25, 28, 30, 40].

Moreover, the handful of models for dielectric elastomers (accounting for dissipative phenomena) that have been proposed in the literature over the past few years following different *ad hoc* approaches are all special cases of the above two-potential framework, that is, they can be readily generated by appropriate choices of the free-energy functions ψ^{Eq}, ψ^{NEq} and the dissipation potential ϕ. As noted in the Introduction, however, the majority of such models account only for mechanical dissipation and, save for a few works [5, 46], most further assume ideal dielectric behavior [2, 18, 47, 51]. Two exemptions that account for both mechanical and electric dissipation are the models presented in [10] and [38].

3 A specific constitutive model for isotropic incompressible dielectric elastomers

In the sequel, we employ the general two-potential constitutive framework laid out in the preceding

section to construct a specific model for the prominent class of isotropic and incompressible dielectric elastomers.

The proposed model corresponds to a generalization of the viscoelastic model of Kumar and Lopez-Pamies [24]—which accounts for the non-Gaussian elasticity and the deformation-enhanced shear-thinning viscosity typical of elastomers [1, 12, 21, 31]—aimed at accounting for the time- and deformation-dependent polarization and electrostriction characteristic of dielectric elastomers [7, 17, 22, 48].

We begin in Sect. 3.1 by presenting the prescriptions for the functions ψ^{Eq}, ψ^{NEq}, ϕ and then present the constitutive response that they imply in Sect. 3.2 together with the key theoretical and practical features of the model. We devote Sect. 3.3 to discussing in detail its specialization in the so-called limit of small deformations and moderate electric fields.

3.1 The functions ψ^{Eq}, ψ^{NEq}, ϕ

The equilibrium free-energy function ψ^{Eq} in the proposed model is given by

$$\psi^{\text{Eq}} = \begin{cases} \psi^{\text{Eq}}_{\text{LP}}(I_1) + \dfrac{m_{\text{K}} - \varepsilon}{2} I_4 - \dfrac{m_{\text{K}}}{2} I_5 & \text{if} \quad J = 1 \\ +\infty & \text{otherwise} \end{cases} \tag{17}$$

with

$$\psi^{\text{Eq}}_{\text{LP}}(I_1) = \sum_{r=1}^{2} \frac{3^{1-\alpha_r}}{2\alpha_r} \mu_r \left[I_1^{\alpha_r} - 3^{\alpha_r} \right],$$

where I_1, I_4, I_5 stand for the standard invariants

$$I_1 = \text{tr}\, \mathbf{C}, \quad I_4 = \mathbf{E} \cdot \mathbf{E}, \quad I_5 = \mathbf{E} \cdot \mathbf{C}^{-1} \mathbf{E},$$

written here in terms of the right Cauchy-Green deformation tensor $\mathbf{C} = \mathbf{F}^T \mathbf{F}$, and where μ_r, α_r $(r = 1, 2)$ stand for the material parameters (with unit *force*/*length*^{2} and unitless) describing the elasticity of the dielectric elastomer at states of mechanical and electric equilibrium, while the material parameters ε and m_{K} denote, respectively, its initial permittivity and electrostriction coefficient (both with units *capacitance*/*length*), also at equilibrium states.

Remark 6 It is a simple matter to check that the equilibrium free-energy function (17) satisfies the requirements of even electromechanical coupling $(7)_1$, material frame indifference $(8)_1$, and material symmetry $(9)_1$ for the case of isotropic dielectric elastomers of interest here.

The non-equilibrium free-energy function ψ^{NEq} is taken to be given by the same functional form as the equilibrium free energy (17) evaluated at appropriate deformation-gradient and electric-field arguments compliant with the constraints $(7)_2$, $(8)_2$, $(9)_2$. Specifically,

$$\psi^{\text{NEq}} = \begin{cases} \psi^{\text{NEq}}_{\text{LP}}(I_1^e) + \dfrac{n_{\text{K}} - \epsilon}{2} I_4^e - \dfrac{n_{\text{K}}}{2} \mathcal{I}_5^e & \text{if} \quad J^e = 1 \\ +\infty & \text{otherwise} \end{cases} \tag{18}$$

with

$$\psi^{\text{NEq}}_{\text{LP}}(I_1^e) = \sum_{r=1}^{2} \frac{3^{1-\beta_r}}{2\beta_r} \nu_r \left[I_1^{e\beta_r} - 3^{\beta_r} \right],$$

where I_1^e, J^e, I_4^e, $\mathcal{I}_5^e$ stand for the pseudo-invariants

$$\begin{cases} I_1^e = \text{tr}\, \mathbf{C}^e = \mathbf{C} \cdot \mathbf{C}^{v-1} \\ J^e = \det \mathbf{F}^e = \dfrac{J}{J^v} \\ I_4^e = \mathbf{E}^e \cdot \mathbf{E}^e = (\mathbf{E} - \mathbf{E}^v) \cdot (\mathbf{E} - \mathbf{E}^v) \\ \mathcal{I}_5^e = \mathbf{E}^e \cdot \mathbf{C}^{-1} \mathbf{E}^e = (\mathbf{E} - \mathbf{E}^v) \cdot \mathbf{C}^{-1} (\mathbf{E} - \mathbf{E}^v) \end{cases}, . \tag{19}$$

and where ν_1, β_1, ν_2, β_2, ϵ, n_{K} stand for the six material parameters analogous to μ_1, α_1, μ_2, α_2, ε, m_{K} in the equilibrium branch (17); for later use, in these last expressions we have introduced the notation $\mathbf{C}^e = \mathbf{F}^{eT} \mathbf{F}^e$, $\mathbf{C}^v = \mathbf{F}^{vT} \mathbf{F}^v$, $J^v = \det \mathbf{F}^v$.

Remark 7 Similar to (17), it is a simple matter to check that the non-equilibrium free-energy function (18) satisfies the requirements of even electromechanical coupling $(7)_2$, material frame indifference $(8)_2$, and material symmetry $(9)_2$ for $Symm = Orth^+$.

Remark 8 While in principle natural choices as arguments in ψ^{NEq}, the pseudo-invariants $I_5^e = \mathbf{E}^e \cdot \mathbf{C}^{e-1} \mathbf{E}^e$ and $I_6^e = \mathbf{E}^e \cdot \mathbf{C}^{e-2} \mathbf{E}^e$ do *not* satisfy the material symmetry requirement $(9)_2$. On the other hand, the pseudo-invariants $\mathcal{I}_5^e = \mathbf{E}^e \cdot \mathbf{C}^{-1} \mathbf{E}^e$ and $\mathcal{I}_6^e = \mathbf{E}^e \cdot \mathbf{C}^{-2} \mathbf{E}^e$ do satisfy such a constraint, thus the use of $\mathcal{I}_5^e$ in (18).

Finally, the dissipation potential ϕ is prescribed as

$$\phi = \frac{1}{2}\dot{\mathbf{F}}^{v}\mathbf{F}^{v-1}\cdot\left[\boldsymbol{\mathcal{A}}(\mathbf{F},\mathbf{F}^{e})\dot{\mathbf{F}}^{v}\mathbf{F}^{v-1}\right] + \frac{1}{2}\mathbf{F}^{-T}\dot{\mathbf{E}}^{v}\cdot\left[\boldsymbol{\mathcal{B}}(\mathbf{F},\mathbf{E},\mathbf{E}^{e})\mathbf{F}^{-T}\dot{\mathbf{E}}^{v}\right] \tag{20}$$

with

$$\mathcal{A}_{ijkl}(\mathbf{F},\mathbf{F}^{e}) = 2\eta_{\mathrm{K}}(I_1^{e},I_2^{e},I_1^{v})\mathcal{K}_{ijkl} + 3\eta_{\mathrm{J}}\mathcal{J}_{ijkl} \tag{21}$$

and

$$\mathcal{B}_{ij}(\mathbf{F},\mathbf{E},\mathbf{E}^{e}) = \zeta\delta_{ij}, \tag{22}$$

where δ_{ij} denotes the Kronecker delta, and $\mathcal{K}$ and $\mathcal{J}$ stand for the standard shear and hydrostatic orthogonal projection tensors

$$\mathcal{K}_{ijkl} = \frac{1}{2}\left[\delta_{ik}\delta_{jl} + \delta_{il}\delta_{jk} - \frac{2}{3}\delta_{ij}\delta_{kl}\right],\ \mathcal{J}_{ijkl} = \frac{1}{3}\delta_{ij}\delta_{kl}. \tag{23}$$

In the constitutive prescriptions (21)–(22), η_{K}, η_{J}, and ζ are material functions/parameters that describe, respectively, the viscosity and the polarization friction of the dielectric elastomer. The two viscosity coefficients are given by

$$\eta_{\mathrm{K}}(I_1^{e},I_2^{e},I_1^{v}) = \eta_{\infty} + \frac{\eta_0 - \eta_{\infty} + K_1\left[I_1^{v\gamma_1} - 3^{\gamma_1}\right]}{1 + \left(K_2\, J_2^{\mathrm{NEq}}\right)^{\gamma_2}}$$

with

$$J_2^{\mathrm{NEq}} = \left(\frac{I_1^{e\,2}}{3} - I_2^{e}\right)\left(\sum_{r=1}^{2} 3^{1-\beta_r} v_r I_1^{e\,\beta_r - 1}\right)^{2}$$

and

$$\eta_{\mathrm{J}} = +\infty,$$

where we recall that I_1^{e} is given by $(19)_1$ in terms of $\mathbf{C}$ and $\mathbf{C}^{v}$,

$$\begin{cases} I_2^{e} = \frac{1}{2}\left[(\operatorname{tr}\mathbf{C}^{e})^2 - \operatorname{tr}\mathbf{C}^{e2}\right] \\ \quad = \frac{1}{2}\left[(\mathbf{C}\cdot\mathbf{C}^{v-1})^2 - \mathbf{C}^{v-1}\mathbf{C}\cdot\mathbf{C}\mathbf{C}^{v-1}\right], \\ I_1^{v} = \operatorname{tr}\mathbf{C}^{v} \end{cases}$$

and $\eta_0 > \eta_{\infty} \geq 0$, $\gamma_1 \geq 0$, $\gamma_2 \geq 0$, $K_1 \geq 0$, $K_2 \geq 0$ are material parameters; the units of η_{J}, η_0, η_{∞}, K_1 are *force* $\times$ *time*/*length*^{2}, γ_1, γ_2 are unitless, while K_2 has units of *length*^{4}/*force*^{2}. The polarization-friction parameter ζ is taken to be a non-negative material constant with unit *capacitance* $\times$ *time*/*length*.

Remark 9 It is not difficult to verify that the dissipation potential (20) satisfies the requirements of even electromechanical coupling $(7)_3$, material frame indifference $(8)_3$, and material symmetry $(9)_3$ for $Symm = Orth^{+}$. Noting the inequalities $\eta_{\mathrm{K}} \geq 0$, $\eta_{\mathrm{J}} > 0$, $\zeta \geq 0$, it is also straightforward to check that the dissipation potential (20) complies as well with the reduced dissipation inequality (10).

Remark 10 The polarization-friction coefficient ζ in the dissipation potential (20) can be vastly generalized to be a function of the deformation gradient $\mathbf{F}$, the electric field $\mathbf{E}$, and/or the internal variable $\mathbf{E}^{v}$, instead of just a constant. For instance, any (suitably well-behaved) non-negative function of the generic form

$$\zeta = \zeta(I_1, I_4, I_5, I_4^{e}, \mathcal{I}_5^{e})$$

may be employed. Because of the current lack of guiding experimental results, we choose ζ to be a constant in this work.

3.2 The constitutive response

Having introduced the free-energy functions (17) and (18) and the dissipation potential (20), it is now a simple matter to spell out the constitutive relations (3)–(4) with evolution equations (5) that they imply. Indeed, the first Piola-Kirchhoff stress $\mathbf{S}$ and Lagrangian electric displacement $\mathbf{D}$ are given simply by

$$\begin{aligned} \mathbf{S} = &\left[\sum_{r=1}^{2} 3^{1-\alpha_r}\mu_r I_1^{\alpha_r - 1}\right]\mathbf{F} - p\,\mathbf{F}^{-T} \\ &+ \left[\sum_{r=1}^{2} 3^{1-\beta_r} v_r (\mathbf{C}\cdot\mathbf{C}^{v-1})^{\beta_r - 1}\right]\mathbf{F}\mathbf{C}^{v-1} \\ &+ m_{\mathrm{K}}\mathbf{F}^{-T}\mathbf{E}\otimes\mathbf{F}^{-1}\mathbf{F}^{-T}\mathbf{E} \\ &+ n_{\mathrm{K}}\mathbf{F}^{-T}(\mathbf{E}-\mathbf{E}^{v})\otimes\mathbf{F}^{-1}\mathbf{F}^{-T}(\mathbf{E}-\mathbf{E}^{v}) \end{aligned} \tag{24}$$

and

$$\begin{aligned} \mathbf{D} = &(\varepsilon - m_{\mathrm{K}})\mathbf{E} + m_{\mathrm{K}}\mathbf{F}^{-1}\mathbf{F}^{-T}\mathbf{E} \\ &+ (\epsilon - n_{\mathrm{K}})(\mathbf{E}-\mathbf{E}^{v}) + n_{\mathrm{K}}\mathbf{F}^{-1}\mathbf{F}^{-T}(\mathbf{E}-\mathbf{E}^{v}), \end{aligned} \tag{25}$$

where p stands for the arbitrary hydrostatic pressure associated with the incompressibility constraint $J = 1$,

and where $\mathbf{C}^v$ and $\mathbf{E}^v$ are defined implicitly as solutions of the evolution equations

$$\begin{cases} \dot{\mathbf{C}}^v = \dfrac{\sum_{r=1}^{2} 3^{1-\beta_r} \nu_r (\mathbf{C}\cdot\mathbf{C}^{v-1})^{\beta_r-1}}{\eta_{\mathrm{K}}(I_1^e, I_2^e, I_1^v)} \left[\mathbf{C} - \dfrac{1}{3}(\mathbf{C}\cdot\mathbf{C}^{v-1})\mathbf{C}^v\right] \\ \mathbf{C}^v(\mathbf{X},0) = \mathbf{I} \end{cases} \tag{26}$$

and

$$\begin{cases} \dot{\mathbf{E}}^v = -\left(\dfrac{n_{\mathrm{K}}}{\zeta}\mathbf{I} + \dfrac{\epsilon - n_{\mathrm{K}}}{\zeta}\mathbf{C}\right)(\mathbf{E} - \mathbf{E}^v); \\ \mathbf{E}^v(\mathbf{X},0) = \mathbf{0} \end{cases} \tag{27}$$

note that the dependence on the internal variable $\mathbf{F}^v$ enters only through the combination $\mathbf{C}^v = \mathbf{F}^{vT}\mathbf{F}^v$.

The remainder of this section is dedicated to describing key features of the proposed constitutive model (24)–(27).

The Eulerian description. It follows from the constitutive relations (24)–(25) and the connections (6) that the Cauchy stress $\mathbf{T}$ and Eulerian electric displacement $\mathbf{d}$ are given by

$$\begin{aligned} \mathbf{T} = &\left[\sum_{r=1}^{2} 3^{1-\alpha_r}\mu_r I_1^{\alpha_r-1}\right]\mathbf{F}\mathbf{F}^T - p\,\mathbf{I} \\ &+ \left[\sum_{r=1}^{2} 3^{1-\beta_r}\nu_r(\mathbf{C}\cdot\mathbf{C}^{v-1})^{\beta_r-1}\right]\mathbf{F}\mathbf{C}^{v-1}\mathbf{F}^T \\ &+ m_{\mathrm{K}}\mathbf{e}\otimes\mathbf{e} + n_{\mathrm{K}}(\mathbf{e}-\mathbf{e}^v)\otimes(\mathbf{e}-\mathbf{e}^v) \end{aligned}$$

and

$$\begin{aligned} \mathbf{d} = &\left[(\varepsilon - m_{\mathrm{K}})\mathbf{F}\mathbf{F}^T + m_{\mathrm{K}}\mathbf{I}\right]\mathbf{e} \\ &+ \left[(\epsilon - n_{\mathrm{K}})\mathbf{F}\mathbf{F}^T + n_{\mathrm{K}}\mathbf{I}\right](\mathbf{e}-\mathbf{e}^v) \end{aligned} \tag{28}$$

in terms of the Eulerian electric field $\mathbf{e} = \mathbf{F}^{-T}\mathbf{E}$, where use has been made of the notation $\mathbf{e}^v = \mathbf{F}^{-T}\mathbf{E}^v$.

The special case when $\mathbf{E} = \mathbf{E}^v = \mathbf{0}$. In the absence of electric fields when $\mathbf{E} = \mathbf{E}^v = \mathbf{0}$, the model (24)–(27) reduces to the viscoelastic model of Kumar and Lopez-Pamies [24], precisely, the first Piola-Kirchhoff stress (24) reduces to

$$\begin{aligned} \mathbf{S} = &\left[\sum_{r=1}^{2} 3^{1-\alpha_r}\mu_r I_1^{\alpha_r-1}\right]\mathbf{F} - p\,\mathbf{F}^{-T} \\ &+ \left[\sum_{r=1}^{2} 3^{1-\beta_r}\nu_r(\mathbf{C}\cdot\mathbf{C}^{v-1})^{\beta_r-1}\right]\mathbf{F}\mathbf{C}^{v-1}, \end{aligned}$$

where $\mathbf{C}^v$ is still defined by the evolution equation (26). Because such a model accounts for the non-Gaussian elasticity and the deformation-enhanced shear-thinning viscosity typical of elastomers, it is expected to be descriptive and predictive of the viscoelastic behavior of most standard elastomers; see Section 3.1 in [24] for comparisons with experiments.

The special case when $\mathbf{F} = \mathbf{F}^v = \mathbf{Q} \in Orth^+$. In the absence of stretch when $\mathbf{F} = \mathbf{F}^v = \mathbf{Q} \in Orth^+$, the model (24)–(27) reduces to the classical Debye model [8], precisely, the electric displacement (25) reduces to

$$\mathbf{D} = \varepsilon\,\mathbf{E} + \epsilon(\mathbf{E} - \mathbf{E}^v),$$

where $\mathbf{E}^v$ is solution of the evolution equation

$$\begin{cases} \dot{\mathbf{E}}^v = -\dfrac{\epsilon}{\zeta}(\mathbf{E} - \mathbf{E}^v) \\ \mathbf{E}^v(\mathbf{X},0) = \mathbf{0} \end{cases}.$$

This constitutive relation describes reasonably well the time-dependent polarization response of most standard dielectric elastomers all the way up to their electric breakdown; see, e.g., the experimental results presented in [7, 17, 22, 52].

Numerical solution of the evolution equations (26) *and* (27). The evolution equations (26) and (27) for the internal variables $\mathbf{C}^v$ and $\mathbf{E}^v$ are decoupled from one another and hence can be solved independently. Moreover, while the evolution equation (27) for the electric internal variable $\mathbf{E}^v$ does depend on both the deformation and the electric field in the dielectric elastomer via $\mathbf{C}$ and $\mathbf{E}$, the evolution equation (26) for the mechanical internal variable $\mathbf{C}^v$ does *not* depend on $\mathbf{E}$.

From a mathematical point of view, both evolution equations are systems of first-order ODEs. Whereas the system (27) for $\mathbf{E}^v$ is linear, the system (26) for $\mathbf{C}^v$ is nonlinear. An efficient and robust[2] numerical scheme to generate solutions for both of these systems is the explicit fifth-order Runge-Kutta scheme with extended region of stability due to Lawson [25]. For a generic system of nonlinear first-order ODEs

[2] Numerical experiments have shown that this scheme remains stable and accurate over very long times, while, at the same time, it also outperforms in terms of computational cost all of the various implicit methods that we have examined.

$$\dot{\mathbf{A}}(t) = \mathbf{G}(t, \mathbf{A}(t)),$$

denoting by $\mathbf{A}_k$ the numerical approximation of the solution $\mathbf{A}(t_k)$ at the discretized time t_k, this scheme provides the solution $\mathbf{A}_{n+1}$ in terms of the solution at the previous time step $\mathbf{A}_n$, for a given discretized time interval $[t_n, t_{n+1}]$, by the rule

$$\mathbf{A}_{n+1} = \mathbf{A}_n + \frac{\Delta t}{90}(7\mathbf{k}_1 + 32\mathbf{k}_3 + 12\mathbf{k}_4 + 32\mathbf{k}_5 + 7\mathbf{k}_6)$$

with

$$\begin{aligned}
\mathbf{k}_1 &= \mathbf{G}(t_n, \mathbf{A}_n)\\
\mathbf{k}_2 &= \mathbf{G}\left(t_n + \frac{\Delta t}{2}, \mathbf{A}_n + \mathbf{k}_1 \frac{\Delta t}{2}\right)\\
\mathbf{k}_3 &= \mathbf{G}\left(t_n + \frac{\Delta t}{4}, \mathbf{A}_n + (3\mathbf{k}_1 + \mathbf{k}_2) \frac{\Delta t}{16}\right)\\
\mathbf{k}_4 &= \mathbf{G}\left(t_n + \frac{\Delta t}{2}, \mathbf{A}_n + \mathbf{k}_3 \frac{\Delta t}{2}\right)\\
\mathbf{k}_5 &= \mathbf{G}\left(t_n + \frac{3\Delta t}{4}, \mathbf{A}_n + 3(-\mathbf{k}_2 + 2\mathbf{k}_3 + 3\mathbf{k}_4) \frac{\Delta t}{16}\right)\\
\mathbf{k}_6 &= \mathbf{G}\left(t_n + \Delta t, \mathbf{A}_n + (\mathbf{k}_1 + 4\mathbf{k}_2 + 6\mathbf{k}_3 - 12\mathbf{k}_4 + 8\mathbf{k}_5) \frac{\Delta t}{7}\right),
\end{aligned}$$

where $\Delta t = t_{n+1} - t_n$.

Material parameters and their determination from experiments. The model (24)–(27) contains nineteen material parameters:

- four (μ_1, α_1, μ_2, α_2) describing the non-Gaussian elasticity at states of mechanical and electric equilibrium,
- four (ν_1, β_1, ν_2, β_2) describing the additional non-Gaussian elasticity at non-equilibrium states,
- six (η_0, η_∞, γ_1, γ_2, K_1, K_2) describing the viscous dissipation that stems from the motion of the underlying polymer chains,
- two (ε, m_{K}) describing the polarization and electrostriction at states of mechanical and electric equilibrium,
- two (ϵ, n_{K}) describing the additional polarization and electrostriction at non-equilibrium states, and
- one (ζ) describing the frictional dissipation that stems from the process of polarization.

The fourteen purely mechanical parameters (μ_1, α_1, μ_2, α_2, ν_1, β_1, ν_2, β_2, η_0, η_∞, γ_1, γ_2, K_1, K_2) can be determined by simply fitting (e.g., by means of least squares) the model simultaneously to a set of uniaxial relaxation data and a set of uniaxial tension/compression data at constant stretch rate. Alternatively, they can be determined by fitting simultaneously two sets of uniaxial tension/compression data at two sufficiently different constant deformation rates; see Section 3.1 in [24].

The three purely electric parameters (ε, ϵ, ζ) can be determined from conventional broadband dielectric spectroscopy measurements; see, e.g., Chapter 2 in [23].

Finally, the two remaining electromechanical parameters (m_{K}, n_{K}) can be determined from electrostriction experiments and from broadband dielectric spectroscopy measurements in pre-stretched specimens; see, e.g., [22, 28, 37, 48].

Dielectric spectroscopy on pre-stretched specimens. As just mentioned, a standard experimental technique to probe the electromechanical behavior of dielectric elastomers is the dielectric spectroscopy of pre-stretched specimens.

Customarily, as a first step, a thin layer of the dielectric elastomer of interest is stretched biaxially, say λ_1 in the $\mathbf{e}_1$ direction and λ_2 in the perpendicular direction $\mathbf{e}_2$, and held in place for long enough (usually, about a day) to reach mechanical equilibrium so that, according to the model (24)–(27), the deformation gradient $\mathbf{F}$ and internal variable $\mathbf{C}^v$ are of the spatially homogeneous and constant-in-time forms

$$F_{ij} = \begin{bmatrix} \lambda_1 & 0 & 0 \\ 0 & \lambda_2 & 0 \\ 0 & 0 & \dfrac{1}{\lambda_1\lambda_2} \end{bmatrix}$$
$$\text{and} \quad C^v_{ij} = C_{ij} = \begin{bmatrix} \lambda_1^2 & 0 & 0 \\ 0 & \lambda_2^2 & 0 \\ 0 & 0 & \dfrac{1}{\lambda_1^2\lambda_2^2} \end{bmatrix} \tag{29}$$

with respect to the Cartesian laboratory axes $\{\mathbf{e}_1, \mathbf{e}_2, \mathbf{e}_3\}$, where $\mathbf{e}_3$ denotes the thin layer normal.

Keeping the stretched configuration (29) fixed, as a second step, electrodes are placed on the opposite surfaces of the specimen and these are then connected to a power source that sets a time-harmonic voltage across. Neglecting fringe effects, the Lagrangian electric field $\mathbf{E}$ and internal variable $\mathbf{E}^v$ in the specimen specialize to be of the forms

$$E_i = \begin{bmatrix} 0 \\ 0 \\ E(t) \end{bmatrix} \quad \text{with} \quad E(t) = E_0 e^{i\omega t} \tag{30}$$

and

$$E_i^v = \begin{bmatrix} 0 \\ 0 \\ E^v(t) \end{bmatrix} \quad \text{with} \quad E^v(t) = \frac{E_0}{1+i\omega\tau}\left(e^{i\omega t} - e^{-\frac{t}{\tau}}\right), \tag{31}$$

where ω is the angular frequency of the applied harmonic voltage, $i = \sqrt{-1}$, E_0 is the amplitude of the induced Lagrangian electric field, and

$$\tau = \frac{\lambda_1^2\lambda_2^2\zeta}{(1-\lambda_1^2\lambda_2^2)n_{\rm K} - \epsilon} \tag{32}$$

has been introduced for notational convenience. Physically, this last quantity characterizes the electric relaxation time of the dielectric elastomer at the stretched configuration (29).

The third and last step consists in running the experiment for a sufficiently long period of time (usually, a few miliseconds suffice) so that the initial transient part of the response—characterized by the term $e^{-\frac{t}{\tau}}$ in (31)—vanishes and a harmonic relationship can be established between the Eulerian electric displacement $\mathbf{d} = \mathbf{F}\mathbf{D} = d(t)\mathbf{e}_3$ and the Eulerian electric field $\mathbf{e} = \mathbf{F}^{-T}\mathbf{E} = \lambda_1\lambda_2 E_0 e^{i\omega t}\mathbf{e}_3 = e_0 e^{i\omega t}\mathbf{e}_3$. It immediately follows from (28), $(29)_1$, (30), and (31) that that harmonic relationship is given by

$$d(t) = \varepsilon^\star(\omega;\lambda_1,\lambda_2)e_0 e^{i\omega t}$$

with

$$\varepsilon^\star(\omega;\lambda_1,\lambda_2) = m_{\rm K} + n_{\rm K} + \frac{\varepsilon+\epsilon-m_{\rm K}-n_{\rm K}}{\lambda_1^2\lambda_2^2} - \frac{1}{1+i\omega\tau}\left(n_{\rm K} + \frac{\epsilon-n_{\rm K}}{\lambda_1^2\lambda_2^2}\right). \tag{33}$$

Clearly, the quantity (33) can be thought of as the apparent permittivity of the dielectric elastomer at the stretched configuration (29) and this is how (33) is precisely interpreted in the experimental literature. Using the convention $\varepsilon^\star(\omega;\lambda_1,\lambda_2) = \varepsilon^{\star\prime}(\omega;\lambda_1,\lambda_2) - i\varepsilon^{\star\prime\prime}(\omega;\lambda_1,\lambda_2)$, its real $\varepsilon^{\star\prime}(\omega;\lambda_1,\lambda_2)$ and imaginary $\varepsilon^{\star\prime\prime}(\omega;\lambda_1,\lambda_2)$ parts read as

$$\varepsilon^{\star\prime}(\omega;\lambda_1,\lambda_2) = m_{\rm K} + n_{\rm K} + \frac{\varepsilon+\epsilon-m_{\rm K}-n_{\rm K}}{\lambda_1^2\lambda_2^2} - \frac{1}{1+\omega^2\tau^2}\left(n_{\rm K} + \frac{\epsilon-n_{\rm K}}{\lambda_1^2\lambda_2^2}\right) \tag{34}$$

and

$$\varepsilon^{\star\prime\prime}(\omega;\lambda_1,\lambda_2) = -\frac{\omega\tau}{1+\omega^2\tau^2}\left(n_{\rm K} + \frac{\epsilon-n_{\rm K}}{\lambda_1^2\lambda_2^2}\right), \tag{35}$$

where we recall that τ is given by (32). Relations (34)–(35) make it plain that the dielectric spectroscopy of pre-stretched specimens is indeed an expedient approach to determine the electromechanical material parameters $m_{\rm K}$ and $n_{\rm K}$ of any dielectric elastomer of interest. Section 4 below presents an example of such a calibration process for the acrylate elastomer VHB 4910.

3.3 The limit of small deformations and moderate electric fields

The distinguishing *even* electromechanical coupling of dielectric elastomers comes forth most plainly in the so-called limit of small deformations and moderate electric fields. Such a limit has been studied extensively in the restricted setting of elastic dielectrics, when both mechanical and electric dissipation are absent; see, e.g., [26, 41, 42, 44, 45]. In this subsection, we work out the limit of small deformations and moderate electric fields for the proposed model (24)–(27) in the general setting when mechanical and electric dissipation are both present.

Consider ξ to be a non-negative scalar parameter of choice and take the deformation gradient and the Lagrangian electric field to be of the orders $||\mathbf{F}-\mathbf{I}|| = O(\xi)$ and $||\mathbf{E}|| = O(\xi^{\frac{1}{2}})$. In the limit as $\xi \searrow 0$, making use of the notation $\mathbf{H} = \mathbf{F} - \mathbf{I}$ and $\mathbf{H}^v = \mathbf{F}^v - \mathbf{I}$, it follows that the constitutive response (24)–(27) reduces asymptotically to leading order to

$$\mathbf{S} = \mathbf{L}^{\rm Eq}\mathbf{H} + \mathbf{L}^{\rm NEq}(\mathbf{H}-\mathbf{H}^v) - p\mathbf{I} + \mathbf{M}^{\rm Eq}\mathbf{E}\otimes\mathbf{E} + \mathbf{M}^{\rm NEq}(\mathbf{E}-\mathbf{E}^v)\otimes(\mathbf{E}-\mathbf{E}^v), \tag{36}$$

subject to the constraint $\operatorname{tr}\mathbf{H} = 0$, and

$$\mathbf{D} = \boldsymbol{\varepsilon}^{\mathrm{Eq}}\mathbf{E} + \boldsymbol{\varepsilon}^{\mathrm{NEq}}(\mathbf{E} - \mathbf{E}^{v}) \tag{37}$$

with

$$\begin{aligned} &\mathbf{L}^{\mathrm{Eq}} = 2(\mu_1 + \mu_2)\mathcal{K}, \quad \mathbf{L}^{\mathrm{NEq}} = 2(v_1 + v_2)\mathcal{K}, \\ &\mathbf{M}^{\mathrm{Eq}} = m_{\mathrm{K}}(\mathcal{K} + \mathcal{J}), \quad \mathbf{M}^{\mathrm{NEq}} = n_{\mathrm{K}}(\mathcal{K} + \mathcal{J}), \\ &\boldsymbol{\varepsilon}^{\mathrm{Eq}} = \varepsilon\,\mathbf{I}, \quad \boldsymbol{\varepsilon}^{\mathrm{NEq}} = \epsilon\,\mathbf{I}, \end{aligned} \tag{38}$$

where p stands for the arbitrary hydrostatic pressure associated with the incompressibility constraint $\mathrm{tr}\,\mathbf{H} = 0$, $\mathcal{K}$ and $\mathcal{J}$ stand, again, for the orthogonal projection tensors (23), and $\mathbf{H}^{v}$ and $\mathbf{E}^{v}$ are defined by the evolution equations

$$\begin{cases} \dot{\mathbf{H}}^{v} = \dfrac{v_1 + v_2}{\eta_0}(\mathbf{H} - \mathbf{H}^{v}) \\ \mathbf{H}^{v}(\mathbf{X}, 0) = \mathbf{0} \end{cases}$$

and

$$\begin{cases} \dot{\mathbf{E}}^{v} = -\dfrac{\epsilon}{\zeta}(\mathbf{E} - \mathbf{E}^{v}) \\ \mathbf{E}^{v}(\mathbf{X}, 0) = \mathbf{0} \end{cases},$$

which admit the closed-form solutions

$$H^{v}_{ij}(\mathbf{X}, t) = \int_0^t \frac{e^{-\frac{t-s}{\tau_{\mathtt{m}}}}}{\tau_{\mathtt{m}}} H_{ij}(\mathbf{X}, s)\mathrm{d}s \tag{39}$$

and

$$E^{v}_{i}(\mathbf{X}, t) = \int_0^t \frac{e^{-\frac{t-s}{\tau_{\mathtt{e}}}}}{\tau_{\mathtt{e}}} E_{i}(\mathbf{X}, s)\mathrm{d}s. \tag{40}$$

In these last expressions, we have introduced the notation $\tau_{\mathtt{m}} = \eta_0/(v_1 + v_2)$ and $\tau_{\mathtt{e}} = -\zeta/\epsilon$. Physically, these quantities characterize the mechanical and electric relaxation times of the dielectric elastomer in the limit of small deformations and moderate electric fields. Typically, $\tau_{\mathtt{m}}$ is in the order of 10^2 seconds, while $\tau_{\mathtt{e}}$ is in the much faster range of $[10^{-6}, 10^{-3}]$ seconds.

Reduced set of material parameters. Out of the total of nineteen in the full model (24)–(27), only a combination of eight material parameters shows up in the asymptotic constitutive response (36)–(40):

- one ($\mu = \mu_1 + \mu_2$) describing the initial shear modulus at states of mechanical and electric equilibrium,
- one ($v = v_1 + v_2$) describing the additional initial shear modulus at non-equilibrium states,
- one ($\tau_{\mathtt{m}} = \eta_0/(v_1 + v_2)$) describing the initial mechanical relaxation time,
- two (ε, m_{K}) describing the initial permittivity and electrostriction at states of mechanical and electric equilibrium,
- two (ϵ, n_{K}) describing the additional initial permittivity and electrostriction at non-equilibrium states, and
- one ($\tau_{\mathtt{e}} = -\zeta/\epsilon$) describing the initial electric relaxation time.

Electrostriction. As alluded to above, a fairly accessible and thus popular experiment to probe the coupled electromechanical behavior of dielectric elastomers consists in measuring their deformation—commonly referred to as electrostriction—that results from an imposed spatially homogeneous electric field in the absence of stresses. This is routinely achieved by sandwiching a thin layer of the dielectric elastomer between two compliant electrodes connected to a battery. In such a setup, the stress is indeed roughly zero everywhere (inside the dielectric elastomer as well as in the surrounding space), while the electric field is roughly uniform within the dielectric elastomer and zero outside of it.

Consider hence a thin layer of dielectric elastomer subject to electromechanical states where the stress $\mathbf{S}$ and electric field $\mathbf{E}$ are of the spatially homogeneous—albeit time dependent—forms

$$S_{ij} = \begin{bmatrix} 0 & 0 & 0 \\ 0 & 0 & 0 \\ 0 & 0 & 0 \end{bmatrix} \quad \text{and} \quad E_i = \begin{bmatrix} 0 \\ 0 \\ E(t) \end{bmatrix}$$

with respect to some Cartesian laboratory axes $\{\mathbf{e}_1, \mathbf{e}_2, \mathbf{e}_3\}$, where, as in the preceding section, $\mathbf{e}_3$ denotes the thin layer normal.

It follows from the constitutive relations (36) through (40) that

$$H_{ij} = \begin{bmatrix} -\frac{1}{2}H(t) & 0 & 0 \\ 0 & -\frac{1}{2}H(t) & 0 \\ 0 & 0 & H(t) \end{bmatrix}$$

$$\text{and} \quad D_i = \begin{bmatrix} 0 \\ 0 \\ D(t) \end{bmatrix},$$

where the electrostriction strain $H(t)$ in the direction of the applied electric field is defined implicitly by the Volterra integral equation

$$S_{33} = (\mu_1 + \mu_2 + \nu_1 + \nu_2)H(t) + \frac{m_{\mathrm{K}}}{3}E^2(t) - (\nu_1 + \nu_2)\int_0^t \frac{e^{-\frac{t-s}{\tau_{\mathrm{m}}}}}{\tau_{\mathrm{m}}}H(s)\mathrm{d}s + \frac{n_{\mathrm{K}}}{3}\left(E(t) - \int_0^t \frac{e^{-\frac{t-s}{\tau_{\mathrm{e}}}}}{\tau_{\mathrm{e}}}E(s)\mathrm{d}s\right)^2 = 0, \tag{41}$$

while the sole non-trivial component $D(t)$ of the Lagrangian electric displacement is given explicitly by the relation

$$D(t) = (\varepsilon + \epsilon)E(t) - \epsilon\int_0^t \frac{e^{-\frac{t-s}{\tau_e}}}{\tau_{\mathrm{e}}}E(s)\mathrm{d}s.$$

The result (41) generalizes the classical result for the electrostriction of elastic dielectrics with even electromechanical coupling to account for both mechanical and electric dissipation. Indeed, for the case of applied electric fields $E(t)$ with a fixed constant value for times larger than a certain threshold time, say $E(t) = E_{\mathrm{f}}$ for $t \geq t_{\mathrm{f}}$, the electrostriction strain $H(t)$ defined by (41) reduces asymptotically to the classical result (see, e.g., Section 2.25 in [42] and Eq. (60) in [41])

$$H(t) = H_{\mathrm{f}} = -\frac{m_{\mathrm{K}}}{3(\mu_1 + \mu_2)}E_{\mathrm{f}}^2$$

for $t \gg t_{\mathrm{f}}$, once the mechanical and electric dissipation has taken place and the dielectric elastomer has reached its equilibrium state.

4 Application to VHB 4910

In this last section, for demonstration purposes, we determine the material parameters in the proposed model (24)–(27) for the acrylate elastomer VHB 4910 from 3M by fitting experimental data available in the literature. To illustrate the model's predictive capabilities, we also present comparisons between its predictions and additional experimental data.

Due in part to its growing commercial significance, a plurality of experimental works aimed at characterizing different aspects of the electromechanical behavior of such a dielectric elastomer have been reported in the literature over the past fifteen years. Presumably because of the technical difficulties in carrying out the experiments, however, the reported results are not entirely consistent with one another. Here, for definiteness, we choose subsets of the experimental data reported in [19] and [37] in order to determine the nineteen material parameters in (24)–(27).

Precisely, we make use of the results reported in [19] for the equilibrium states in a multi-step relaxation test together with those from two uniaxial tension loading/unloading tests at the constant stretch rates of 0.01 and 0.05 s^{-1} in order to determine the fourteen purely mechanical parameters (μ_1, α_1, μ_2, α_2, ν_1, β_1, ν_2, β_2, η_0, η_∞, γ_1, γ_2, K_1, K_2) in the model. The resulting values from such a calibration process are listed in Table 1. Figures 5(a)–(b) in [24] compare the three sets of experimental data and the fitted response described by the model.

Furthermore, we make use of the dielectric spectroscopy results reported in [37] for an undeformed specimen and a biaxially pre-stretched specimen, with an equal biaxial stretch of 2, in order to determine the remaining three purely electric parameters (ε, ϵ, ζ) and

Table 1 Material parameters for VHB 4910 determined from experiments in [19] and [37]

$\mu_1 = 13.54\,\mathrm{kPa}$	$\mu_2 = 1.08\,\mathrm{kPa}$
$\alpha_1 = 1.00$	$\alpha_2 = -2.474$
$\nu_1 = 5.42\,\mathrm{kPa}$	$\nu_2 = 20.78\,\mathrm{kPa}$
$\beta_1 = -10$	$\beta_2 = 1.948$
$\eta_0 = 7014\,\mathrm{kPa}\cdot\mathrm{s}$	$\eta_\infty = 0.1\,\mathrm{kPa}\cdot\mathrm{s}$
$\gamma_1 = 1.852$	$\gamma_2 = 0.26$
$K_1 = 3507\,\mathrm{kPa}\cdot\mathrm{s}$	$K_2 = 1\,\mathrm{kPa}^{-2}$
$\varepsilon = 4.48\varepsilon_0$	$m_{\mathrm{K}} = 3.08\varepsilon_0$
$\epsilon = -2.68\varepsilon_0$	$n_{\mathrm{K}} = -0.2788\varepsilon_0$
$\zeta = 3.69\varepsilon_0 \times 10^{-6}\,\mathrm{s}$	

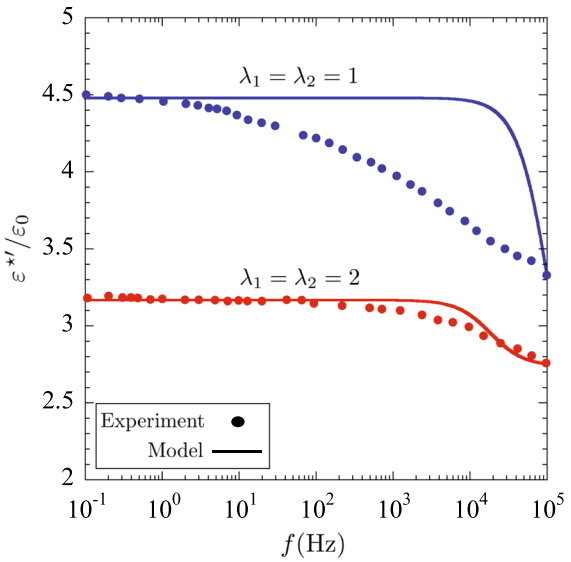

Fig. 2 The model response (34) fitted to the experimental dielectric spectroscopy data of Qiang et al. [37] for the real part of the apparent permittivity of undeformed ($\lambda_1 = \lambda_2 = 1$) and biaxially stretched ($\lambda_1 = \lambda_2 = 2$) VHB 4910 specimens. The results are shown as functions of the frequency $f = \omega/2\pi$, from $f = 0.1$ to 10^5 Hz

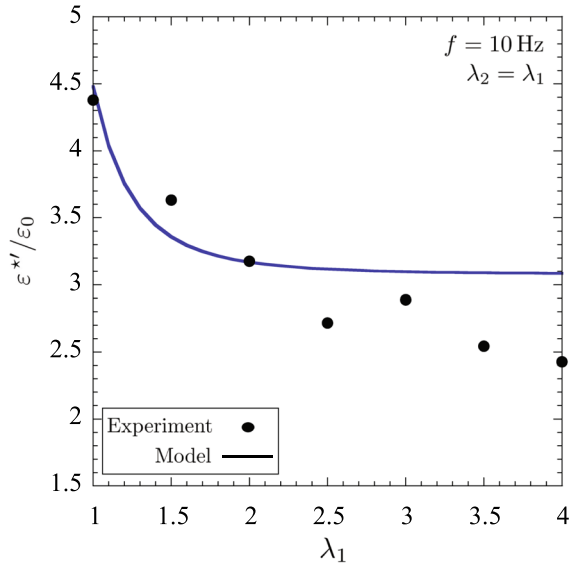

Fig. 3 Real part of the apparent permittivity of biaxially pre-stretched ($\lambda_2 = \lambda_1$) VHB 4910, at the frequency $f = \omega/2\pi = 10$ Hz, as a function of the pre-stretch λ_1. The solid circles correspond to the experimental data of Qiang et al. [37], while the solid line corresponds to the response (34) predicted by the model with the material parameters listed in Table 1

the two electromechanical parameters (m_K, n_K). The results of such a calibration process are also reported in Table 1. Figure 2 compares those two sets of experimental data and the fitted response described by the model. There it is of note that the experimental data for intermediate frequencies is not accurately captured by the model suggesting that the polarization-friction coefficient ζ should not be assumed to simply be constant but rather a function of the electric field $\mathbf{E}$. We shall explore this generalization in future work.

The results presented by Figs. 5(c) and (d) in [24] have already shown that the model (24)–(27) with the material parameters listed in Table 1 can predict the purely mechanical response of VHB 4910 reasonably well. The results presented by Figs. 3 and 4 here indicate that this is also the case more generally for its coupled electromechanical response.

Specifically, Fig. 3 confronts the response (34) predicted by the model with the experimental data of Qiang et al. [37] for the real part of the apparent permittivity of biaxially pre-stretched ($\lambda_2 = \lambda_1 = 1, 1.5, 2, 2.5, 3, 3.5$, and 4) VHB 4910 specimens at the frequency $f = \omega/2\pi = 10$ Hz; see Fig. 6 in [37].

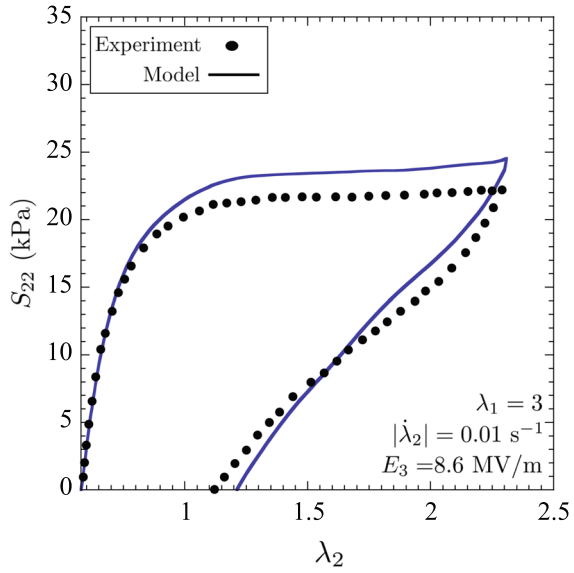

Fig. 4 Load/unload response of uniaxially pre-stretched ($\lambda_1 = 3$) VHB 4910 subject simultaneously to a uniaxial stretch λ_2 perpendicular to the pre-stretch direction, applied at the constant stretch rate of $|\dot{\lambda}_2| = 0.01$ s^{-1}, and a constant Lagrangian electric field $E_3 = 8.6$ MV/m. The solid circles correspond to the experimental data of Hossain et al. [20], while the solid line corresponds to the response predicted by the model with the material parameters listed in Table 1

On the other hand, Fig. 4 compares the model prediction with the experimental data of Hossain et al. [20] for the stress-stretch (S_{22}–λ_2) response of a uniaxially pre-stretched ($\lambda_1 = 3$) specimen that is loaded/unloaded in the direction perpendicular to the pre-stretch at the constant stretch rate of 0.01 s^{-1} in the presence of a 5 kV voltage applied across its thickness resulting in a constant Lagrangian electric field of $E_3 = 8.6$ MV/m; see Fig. 5 in [20].

Funding This work was supported by the National Science Foundation through Grants CMMI–1661853 and DMREF–1922371.

Compliance with ethical standards

Conflict of interest The authors declare that they have no conflict of interest.

Appendix. The reduced dissipation inequality

Denote by $\mathbf{v}(\mathbf{x}, t)$ the velocity of the material point that occupies the location $\mathbf{x} \in \Omega(t)$ at time $t \in [0, T]$ and assume that at any $\mathbf{x} \in \Omega(t)$ and time $t \in [0, T]$ the following quantities exist and are sufficiently regular both in space and time: the mass density $\rho(\mathbf{x}, t)$, the mechanical Cauchy stress $\mathbf{T}^m(\mathbf{x}, t)$, the mechanical body force $\mathbf{f}^m(\mathbf{x}, t)$ (per unit volume), the electric force $\mathbf{f}^e(\mathbf{x}, t)$ (per unit volume), the electric couple $\mathbf{g}^e(\mathbf{x}, t)$ (per unit volume), the electric field $\mathbf{e}(\mathbf{x}, t)$, the electric displacement $\mathbf{d}(\mathbf{x}, t)$, the space charge $q(\mathbf{x}, t)$ (per unit volume), the internal energy $u(\mathbf{x}, t)$ (per unit mass), the heat source $r(\mathbf{x}, t)$ (per unit mass), the heat flux $\widetilde{\mathbf{q}}(\mathbf{x}, t)$, the entropy $\eta(\mathbf{x}, t)$ (per unit mass), and the absolute temperature $\theta(\mathbf{x}, t)$.

Conservation of mass

Conservation of mass is said to be satisfied provided that

$$\frac{\partial \rho}{\partial t} + \operatorname{div}(\rho \mathbf{v}) = 0, \quad (\mathbf{x}, t) \in \Omega(t) \times [0, T]. \tag{A.1}$$

Balance of linear and angular momenta

Absent inertia, the balance of linear and angular momenta are said to be satisfied provided that

$$\operatorname{div} \mathbf{T}^m + \mathbf{f}^m + \mathbf{f}^e = \mathbf{0}, \quad (\mathbf{x}, t) \in \Omega(t) \times [0, T] \tag{A.2}$$

and

$$\widetilde{\boldsymbol{\varepsilon}}\, \mathbf{T}^{mT} = \mathbf{g}^e, \quad (\mathbf{x}, t) \in \Omega(t) \times [0, T], \tag{A.3}$$

where $\widetilde{\boldsymbol{\varepsilon}}$ stands for the permutation symbol.

In the context of electro-quasi-statics of interest here, the electric force and couple take the form (see, e.g., Eqs. (7.38) and (7.48) in [35])

$$\mathbf{f}^e = q\mathbf{e} + (\operatorname{grad} \mathbf{e})^T \mathbf{p} \quad \text{and} \quad \mathbf{g}^e = -\mathbf{p} \times \mathbf{e},$$

where we recall that $\mathbf{p} = \mathbf{d} - \varepsilon_0 \mathbf{e}$ stands for the polarization.

Upon defining the electric stress

$$\mathbf{T}^e = \mathbf{e} \otimes \mathbf{d} - \frac{\varepsilon_0}{2} (\mathbf{e} \cdot \mathbf{e}) \mathbf{I}$$

and invoking Gauss's (A.6) and Faraday's (A.7) laws introduced further below, the balance of linear (A.2) and angular (A.3) momenta can be recast as

$$\operatorname{div} \mathbf{T} + \mathbf{f}^m = \mathbf{0}, \quad (\mathbf{x}, t) \in \Omega(t) \times [0, T] \tag{A.4}$$

and

$$\mathbf{T} = \mathbf{T}^T, \quad (\mathbf{x}, t) \in \Omega(t) \times [0, T] \tag{A.5}$$

in terms of the total Cauchy stress $\mathbf{T} = \mathbf{T}^m + \mathbf{T}^e$. With help of the connections (6) and the definition $\mathbf{f} = J\mathbf{f}^m$, Eqs. (A.4)–(A.5) can be further recast as those summoned in the main body of the text, namely, (11).

Maxwell's equations

In the context of electro-quasi-statics of interest here, Maxwell's equations are said to be satisfied provided that

$$\operatorname{div} \mathbf{d} = q, \quad (\mathbf{x}, t) \in \mathbb{R}^3 \times [0, T] \tag{A.6}$$

and

$$\operatorname{curl} \mathbf{e} = \mathbf{0}, \quad (\mathbf{x}, t) \in \mathbb{R}^3 \times [0, T]. \tag{A.7}$$

With help of the connections (6) and the definition $Q = Jq$, Eqs. (A.6)–(A.7) can be recast in the form (12) provided in the main body of the text.

Balance of energy

Granted the balance Eqs. (A.1), (A.2), (A.3), (A.6), (A.7), balance of energy is said to be satisfied provided that

$$\rho\,\dot{u} + \operatorname{div}\widetilde{\mathbf{q}} - \rho\,r - \mathbf{T}^m\cdot\Gamma - \dot{\mathbf{p}}\cdot\mathbf{e} - (\operatorname{tr}\Gamma)\mathbf{p}\cdot\mathbf{e} = 0, \quad (\mathbf{x},t)\in\Omega(t)\times[0,T], \tag{A.8}$$

where $\Gamma = \partial\mathbf{v}(\mathbf{x},t)/\partial\mathbf{x}$ stands for the Eulerian velocity gradient.

Throughout this appendix, a superposed "dot" denotes the material time derivative.

Entropy imbalance

Granted the balance Eq. (A.1), the entropy imbalance is said to be satisfied provided that

$$\rho\,\dot{\eta} + \operatorname{div}\left(\frac{\widetilde{\mathbf{q}}}{\theta}\right) - \frac{\rho\,r}{\theta} \geq 0, \quad (\mathbf{x},t)\in\Omega(t)\times[0,T]. \tag{A.9}$$

Upon defining the free energy (per unit mass)

$$\Psi = u - \theta\eta - \frac{1}{\rho}\mathbf{p}\cdot\mathbf{e}$$

and invoking the balance Eq. (A.8), the entropy imbalance (A.9) can be recast as the reduced dissipation inequality

$$\rho\left(\dot{\Psi} + \eta\dot{\theta}\right) - \mathbf{T}^m\cdot\Gamma + \mathbf{p}\cdot\dot{\mathbf{e}} + \frac{1}{\theta}\widetilde{\mathbf{q}}\cdot(\operatorname{grad}\theta) \leq 0, \quad (\mathbf{x},t)\in\Omega(t)\times[0,T],$$

which, in the context of isothermal processes of interest in this work, specializes to

$$\rho\,\dot{\Psi} - \mathbf{T}^m\cdot\Gamma + \mathbf{p}\cdot\dot{\mathbf{e}} \leq 0, \quad (\mathbf{x},t)\in\Omega(t)\times[0,T]. \tag{A.10}$$

With help of the definition

$$\psi = J\rho\Psi - \frac{\varepsilon_0}{2}J\mathbf{F}^{-T}\mathbf{E}\cdot\mathbf{F}^{-T}\mathbf{E}$$

and the connections (6), the reduced dissipation inequality (A.10) can be further recast as

$$\dot{\psi} - \mathbf{S}\cdot\dot{\mathbf{F}} + \mathbf{D}\cdot\dot{\mathbf{E}} \leq 0, \quad (\mathbf{X},t)\in\Omega_0\times[0,T]. \tag{A.11}$$

Writing now

$$\psi = \psi^{\mathrm{Eq}}(\mathbf{F},\mathbf{E}) + \psi^{\mathrm{NEq}}(\mathbf{F},\mathbf{E},\mathbf{F}\mathbf{F}^{v-1},\mathbf{E}-\mathbf{E}^v)$$

and making use of the connections (3)–(5), the inequality (A.11) reduces finally to the form (10) provided in the main body of the text.

References

1. Amin AFMS, Lion A, Sekita S, Okui Y (2006) Nonlinear dependence of viscosity in modeling the rate-dependent response of natural and high damping rubbers in compression and shear: experimental identification and numerical verification. Int J Plast 22:1610–1657
2. Ask A, Menzel A, Ristinmaa M (2012) Electrostriction in electro-viscoelastic polymers. Mech Mater 50:9–21
3. Bauer S, Bauer-Gogonea S, Graz I, Kaltenbrunner M, Keplinger C, Schwödiauer R (2014) 25th anniversary article: a soft future: from robots and sensor skin to energy harvesters. Adv Mater 26:149–162
4. Böttcher CJF, Bordewijk P (1978) Theory of electric polarization, dielectrics in time-dependent fields, vol II. Elsevier, Amsterdam
5. Büschel A, Klinkel S, Wagner W (2013) Dielectric elastomers—numerical modelling of nonlinear visco-electroelasticity. Int J Numer Methods Eng 93:834–856
6. Carpi F, De Rossi D, Pelrine R, Sommer-Larsen P (2008) Dielectric elastomers as electromechanical transducers. Elsevier, Amsterdam
7. Cole KS, Cole RH (1941) Dispersion and absorption in dielectrics I. Alternating current characteristics. J Phys Chem 9:341–351
8. Debye P (1929) Polar molecules. The Chemical Catalog Company Inc, New York
9. Dorfmann A, Ogden RW (2005) Nonlinear electroelasticity. Acta Mech 174:167–183
10. Foo CC, Cai S, Koh SJA, Bauer S, Suo Z (2012) Model of dissipative dielectric elastomers. J Appl Phys 111:034102
11. Fosdick R, Tang H (2007) Electrodynamics and thermomechanics of material bodies. J Elast 88:255–297
12. Gent AN (1962) Relaxation processes in vulcanized rubber I: relation among stress relaxation, creep, recovery, and hysteresis. J Appl Polym Sci 6:433–441
13. Germain P, Nguyen QS, Suquet P (1983) Continuum thermodynamics. J Appl Mech 50:1010–1020
14. Gross B (1953) Mathematical structure of the theories of viscoelasticity. Hermann, Paris
15. Gupta U, Qin L, Wang Y, Godaba H, Zhu J (2019) Soft robots based on dielectric elastomer actuators: a review. Smart Mater Struct 28:103002
16. Halphen B, Nguyen QS (1975) Sur les matériaux standard généralisés. J Méc 14:39–63

17. Havriliak S, Negami S (1966) A complex plane analysis of α-dispersions in some polymer systems. J Polym Sci C 14:99–117
18. Hong W (2011) Modeling viscoelastic dielectrics. J Mech Phys Solids 59:637–650
19. Hossain M, Vu DK, Steinmann P (2012) Experimental study and numerical modelling of VHB 4910 polymer. Comput Mater Sci 59:65–74
20. Hossain M, Vu DK, Steinmann P (2015) A comprehensive characterization of the electromechanically coupled properties of VHB 4910 polymer. Arch Appl Mech 85:523–537
21. Khan AS, Lopez-Pamies O (2002) Time and temperature dependent response and relaxation of a soft polymer. Int J Plast 18:1359–1372
22. Kofod G, Sommer-Larsen P, Kornbluh R, Pelrine R (2003) Actuation response of polyacrylate dielectric elastomers. J Intell Mater Syst Struct 14:787–793
23. Kremer F (2003) Schönhals A (2003) Broadband dielectric spectroscopy. Springer, Berlin
24. Kumar A, Lopez-Pamies O (2016) On the two-potential constitutive modelling of rubber viscoelastic materials. Comptes Rendus Mecanique 344:102–112
25. Lawson JD (1966) An order five Runge–Kutta process with extended region of stability. SIAM J Numer Anal 3:593–597
26. Lefèvre V, Lopez-Pamies O (2014) The overall elastic dielectric properties of a suspension of spherical particles in rubber: an exact explicit solution in the small-deformation limit. J Appl Phys 116:134106
27. Lefèvre V, Lopez-Pamies O (2017) Nonlinear electroelastic deformations of dielectric elastomer composites: I—ideal elastic dielectrics. J Mech Phys Solids 99:409–437
28. Lefèvre V, Lopez-Pamies O (2017) Nonlinear electroelastic deformations of dielectric elastomer composites: II—non-Gaussian elastic dielectrics. J Mech Phys Solids 99:438–470
29. Lefèvre V, Danas K, Lopez-Pamies O (2017) A general result for the magnetoelastic response of isotropic suspensions of iron and ferrofluid particles in rubber, with applications to spherical and cylindrical specimens. J Mech Phys Solids 107:343–364
30. Lefèvre V, Garnica A, Lopez-Pamies O (2019) A WENO finite-difference scheme for a new class of Hamilton–Jacobi equations in nonlinear solid mechanics. Comput Methods Appl Mech Eng 349:17–44
31. Lopez-Pamies O (2010) A new I_1-based hyperelastic model for rubber elastic materials. C R Méc 338:3–11
32. Lopez-Pamies O (2014) Elastic dielectric composites: theory and application to particle-filled ideal dielectrics. J Mech Phys Solids 64:61–82
33. Maugin GA, Muschik W (1994) Thermodynamics with internal variables. Part II. Applications. J Non-Equilibrium Thermodyn 19:250–289
34. McMeeking RM, Landis CM (2005) Electrostatic forces and stored energy for deformable dielectric materials. J Appl Mech 72:581–590
35. Pao YH (1978) Electromagnetic forces in deformable continua. Mech Today 4:209–305
36. Pei Q, Hu W, McCoul D, Biggs SJ, Stadler D, Carpi F (2016) Dielectric elastomers as EAPs: applications. Springer International Publishing, Berlin
37. Qiang J, Chen H, Li B (2012) Experimental study on the dielectric properties of polyacrylate dielectric elastomer. Smart Mater Struct 21:025006
38. Saxena P, Vu DK, Steinmann P (2014) On rate-dependent dissipation effects in electro-elasticity. Int J Non-Linear Mech 62:1–11
39. Sidoroff F (1974) Un modèle viscoélastique non linéaire avec configuration intermédiaire. J Méc 13:679–713
40. Schröder J, Keip M-A (2012) Two-scale homogenization of electromechanically coupled boundary value problems. Comput Mech 50:229–244
41. Spinelli SA, Lefèvre V, Lopez-Pamies O (2015) Dielectric elastomer composites: a general closed-form solution in the small-deformation limit. J Mech Phys Solids 83:263–284
42. Stratton JS (1941) Electromagnetic theory. McGraw-Hill, New York
43. Suo Z, Zhao X, Greene WH (2008) A nonlinear field theory of deformable dielectrics. J Mech Phys Solids 56:467–486
44. Tian L, Tevet-Deree L, deBotton G, Bhattacharya K (2012) Dielectric elastomer composites. J Mech Phys Solids 60:181–198
45. Toupin RA (1956) The elastic dielectric. J Ration Mech Anal 5:849–915
46. Vogel F, Göktepe S, Steinmann P, Kuhl E (2014) Modeling and simulation of viscous electro-active polymers. Eur J Mech A/Solids 48:112–128
47. Wang S, Decker M, Henann DL, Chester SA (2016) Modeling of dielectric viscoelastomers with application to electromechanical instabilities. J Mech Phys Solids 95:213–229
48. Wissler M, Mazza E (2007) Electromechanical coupling in dielectric elastomer actuators. Sens Actuators A Phys 138:384–393
49. Wu H, Huang Y, Xu F, Duan Y, Yin Z (2016) Energy harvesters for wearable and stretchable electronics: from flexibility to stretchability. Adv Mater 28:9881–9919
50. Zener CM (1948) Elasticity and anelasticity of metals. University of Chicago Press, Chicago
51. Zhao X, Koh SJA, Suo Z (2011) Nonequilibrium thermodynamics of dielectric elastomers. Int J Appl Mech 3:203–217
52. Zhou J, Jiang L, Cai S (2020) Predicting the electrical breakdown strength of elastomers. Extreme Mech Lett 34:100583
53. Ziegler H (1958) An attempt to generalize Onsager's principle, and its significance for rheological problems. Z Angew Math Phys 9b:748–763
54. Ziegler H, Wehrli C (1987) The derivation of constitutive relations from the free energy and the dissipation function. Adv Appl Mech 25:183–238